

ICSV14
Cairns • Australia
9-12 July, 2007



TRANSMISSION OF SOUND IN A LONG ENCLOSURE WITH A “T” INTERSECTION

S. T. So,¹ W. S. Fung,¹ C. W. Leung¹ and K. M. Li²

¹Department of Mechanical Engineering, The Hong Kong Polytechnic University
Hung Hom, Hong Kong

²Ray W. Herrick Laboratories, School of Mechanical Engineering,
Purdue University, IN 47907-2031, USA
mmkml@purdue.edu

Abstract

Bends, T-intersections, U-shape turns and cross-junctions are some variations that can be found frequently in long enclosed spaces. For a receiver located around the bend in the "T" intersection, the total sound pressure consists of contributions from direct, reflected and diffuse sound waves. The direct sound contribution is dominant in the near fields in the region of sight-lines. The reflected sound field becomes more important as the receiver moves farther away from the corner of the intersection. In all cases, the diffracted sound field at the edge of the bend plays a relatively minor role along a long enclosure. The present study examines the transmission of sound along a tunnel with a "T" intersection. The characteristics of the sound fields are investigated theoretically and experimentally. A numerical model, known as an image source method, has been developed for the prediction of sound transmitted around the corner in the "T" intersection. In the numerical scheme, the phase and magnitude of all contributions from the direct and reflected waves have been included in the calculations. Indoor experiments have been carried out in a corridor with a "T" intersection for validating the theoretical formulation. Experimental results and numerical predictions for the transmission of sound of this configuration in a long enclosure are presented in this paper.

1. INTRODUCTION

Sabine [1], Eyring [2] and Millington [3] developed the classical theory of room acoustics for nearly a century ago. However, the classical theory is not applicable in long enclosures. Yamamoto [4], Allen and Berkeley [5], Kuttruff [6], Antonio [8] and many other researchers developed different empirical and theoretical formulae for predicting the reverberation time in these situations. They used numerical modeling, full-scale field measurements and indoor scale model experiments for predicting the sound fields in a long enclosure. Sergeev [9], Barnett [10] showed that the reverberation time of a long enclosure was significantly different from those enclosed spaces in which the diffuse field was a predominant component.

Many numerical models have been developed for the prediction of sound fields in enclosed spaces or long enclosures. Basically, ray-tracing and image-source methods are two

typical models used in the analysis of sound fields. The finite element method and the boundary element method have also been used to predict the sound field in an enclosed space. However, these computational-intensive methods are only restricted to study the low frequency regime. They will not reflect the full picture of the sound fields at the receivers if the noise source contains significant spectral components at high-frequencies.

By using the image source method, Allen and Berkeley [5], Antonio [8] examined the acoustic properties of a small room. Gibbs and Jones [11] calculated the distribution of noise levels in an enclosure. Borish [12] showed that the image source method has a fundamental advantage over the ray tracing method for an arbitrary polyhedron. Dance and Shield [13, 14] introduced the image source method for a non-diffuse space. Gensane and Santon [15] predicted sound fields in rooms of arbitrary shapes. Only a few researchers [7, 16] dealt with the situations other than a straight space. Gibbs and Jones [11], Wang and Bradley [17, 18] analysed the acoustic effectiveness of partition screen barriers in an open plan office; Li and Iu [19, 20, 21] predicted the sound field in narrow street canyons and tunnels. The image source method was used in all of these earlier studies.

In the present study, predictions of sound field in a T-shape enclosure are explored. Experimental studies, which used hardwood boards to construct a “T” model tunnel, were carried out in an anechoic chamber. Extensive field measurements at a 30 meter long T-corridor were also conducted. Comparisons of numerical predictions and experimental measurements are presented.

2. THEORY

The basic idea of the image source method is as follows:

1. establish all elementary sound rays linking the image sources to the receiver,
2. compute the sound field due to each ray path , and
3. sum the contributions from all sound rays to obtain the total sound field.

It is possible to identify two different situations for the propagation of sound in a “T” enclosure. The first situation is the case when the source and receiver are located at the either sides of the T’s horizontal arm, see Figure 1 (a). In this case, a line-of-sight contact can always be maintained between the source and receiver. The second situation corresponds to the case when the source is located at a horizontal arm whilst the receiver is located at the vertical arm (or vice versa) of the “T” enclosure. Figure 1 (b) shows a schematic diagram of the second situation. In this case, there is normally no direct sight-line contact between the source and receiver unless both of them are located close to the T-junction such that they can ‘see’ each other round the bend. In the following paragraphs, we shall examine the computation of sound fields in these two situations.

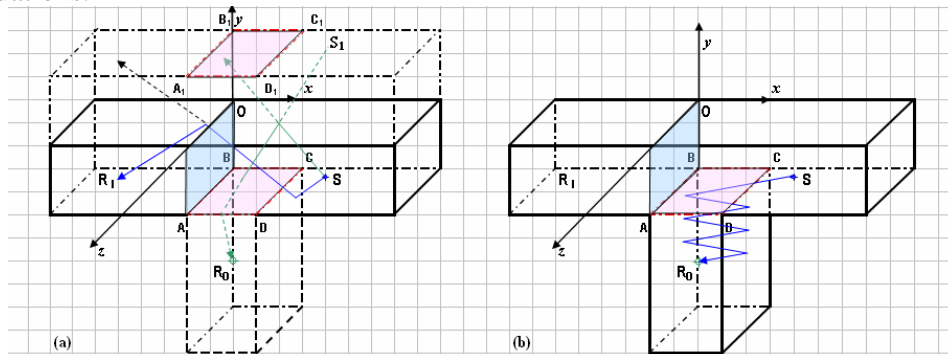


Figure 1: Schematic diagrams showing the source (S) and receiver (R) locating at different parts of a T-enclosure; (a) an in-sight receiver, and (b) an out-of-sight receiver.

2.1 Direct sight-line contact between the source and receiver

As shown in Figure 1(a), the source S is located at the right side of the horizontal arm and the receiver is situated at the left side in which they are separated by the opening ABCD that is connected to the vertical arm of the T-junction. We can treat the opening as a perfect ‘anechoic’ surface. In other words, when a ray hits the boundary area ABCD, all its sound energy will be absorbed with no reflection because the sound ray will be transmitted into the vertical arm of the T-junction through the opening.

To begin the analysis, the image sources are first identified by noting the effect of multiple reflections from the boundary surfaces of the enclosure. A row of image sources is formed by reflections of the two parallel walls from the source. Infinite rows of image sources are then created because of the presence of the reflecting ceiling and ground. The vertical arm of the T-intersection is located at a horizontal distance (in the y -direction) y_t from the source plane with the source and receiver locating at (x_s, y_s, z_s) and (x_r, y_r, z_r) respectively. By considering sound rays emanating from R_t , it is possible to project the opening ABCD and its image on the source plane of $y = 0$. There will be no contributions from the image sources residing in these projected areas because the sound rays (emanating from these image sources) hit the anechoic surface before they can reach the receiver. Hence, the total field is the sum of the remaining image sources that have no interaction with the T-junction.

2.2 No direct sight-line contact between the source and receiver

In this case, the image sources dominate the total sound fields as the source cannot link directly with the receiver. Like the first case, infinite rows of image sources can be formed at the $y = 0$ plane. However, the receiver plane is now perpendicular to the source plane because the receiver is situated at the vertical arm of the T junction. To aid the computation of the sound fields, it is more convenient to introduce image receivers at the receiver plane. We also note that a further plane of image receiver is created because of the parallel wall opposite to the opening ABCD. It is then possible to connect the image sources with the appropriate image receivers in order to establish all possible ray paths linking the image sources with the receiver.

2.3 Prediction of the total fields in a T-junction

With the use of image source method, all possible ray paths connecting the source and receiver can be identified deterministically. The total sound field due to a monopole source of unit strength can then be calculated by summing all contributions coherently to give:

$$P(\omega) = \frac{1}{4\pi} \sum_{n=0}^{\infty} Q_n \frac{e^{ikR_n}}{R_n}, \quad (3)$$

where $k(\equiv \omega/c)$ is the wave number, ω is the angular frequency of the sound source, c is the speed of sound in air, R_n is the distance of the image source n from the receiver, and Q_n is the combined complex wave reflection coefficient associated with the image source n . At each interaction with a boundary surface, the spherical wave reflection coefficient Q is determined according to

$$Q = V + (1 - V)F(w), \quad (4)$$

where V , $F(w)$ and w are the plane wave reflection coefficient, the boundary loss factor and the numerical distance respectively. The computation of these terms can be found elsewhere [22]. The time dependent factor, $e^{-i\omega t}$, is understood and suppressed in the above equation.

In the present study, our attention has been focused on the development of a numerical

model for predicting sound fields in T-junction and its experimental validations. In the subsequent study, the model will be extended to estimate the reverberation time and speech transmission index in such an environment.

3. EXPERIMENTAL VALIDATION OF THE COHERENT MODEL

To present results of the comparison of numerical and experimental, we use the term Relative Sound Pressure Level (RSPL), relative to sound pressure level at 250mm in front of source and excess attenuation (EA), the ratio of the total sound field at various receiver locations to the free field sound pressure at 1 m from the source, i.e.,

$$\text{RSPL} = 10 \log_{10} \left(P(\omega) / P_{ref} \right), \quad (5)$$

$$\text{EA} = 20 \lg (P(\omega)), \quad (6)$$

where $P(\omega)$ is computed according to Eq. (3).

3.1 Indoor model experiments

In the present study, a model T-junction was built with varnished hardwood boards for our experimental measurements. The cross-sectional area, which had dimensions of 610 mm × 580 mm, was the same throughout the enclosure. The horizontal arm of the T-enclosure had an overall length of 5.4 m and the vertical arm had a length of 3.0 m. The model T-enclosure was then placed in an anechoic chamber which had a dimension of 6 m × 6 m × 4 m (height). Experimental data was obtained to validate the theoretical models described in Section 2.

A Brüel and Kjær type 4189 ½" free field microphone and a Tannoy driver were used respectively, as a receiver and a point source. A 25 mm-diameter brass tube of 1.5 m long was connected to the Tannoy driver in order to minimize the reflection of sound the speaker. A PC-based maximum length sequence system analyzer (MLSSA) was used both as a signal generator for the source and as an analyzer for the subsequent processing of data. The maximum length sequence (MLS) technique was chosen in the present study because it has the advantage that no correction of background noise is necessary for a signal to noise ratio of 0 dB. As MLSSA was operated in the time domain where the impulse response was measured, the chosen processing data were based on the time between the arrival of the direct and the last order rays. The time-series data were converted to spectral data by the fast Fourier transform technique. Each spectrum level was then normalized by the pre-recorded direct field measurement taken at 1 m from the source at the free field. The final output was then the Relative Sound Pressure Level (relative to SPL at 250mm in front of the source) spectrum.

The sound pressure level spectrum was measured experimentally at various receiver locations, with the source located 29.5cm above the ground. The source and receiver were located at the centerline of tunnel. In all measurements, the receivers were located at the same height as the source. The horizontal distances between the source and receivers ranged from 0.25 m to 5 m for the sight-line situations. The distance was further extended round the corner along the vertical arm of the T-junction. Figure 2 (a) displays the schematic diagram of the experiments. Figure 2 (b) is a photograph showing the experimental set-up. In order to minimize sound reflection to the receiver, the microphone was clamped on a slender arm on a stand and carried by a trolley. An inextensible nylon string with distance-marker was connected to the trolley at the back of receiving point. The first measuring point, which was the reference, was located at 0.25 m from the source. Every successive point was placed at a separation of 0.25 m. The farthest point was 5 m, for receivers located at the sight-line or non sight-line.

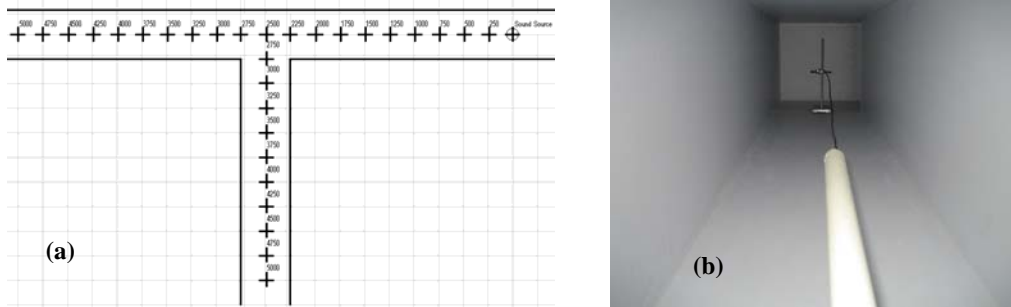


Figure 2: (a) Schematic diagram of the model T-section which has a cross-section area of 610mm x 590mm. It was stationed in an anechoic chamber for the indoor experiments; (b) a photograph showing the experimental set-up with the brass tube at the bottom of the photograph and a stand holding a microphone was located at the top of the photograph.

In Figure 3 (e) – (f), we display comparison of numerical predictions with experimental data for the spectrum of RSPL at six different source/receiver separations either along the line of sight or at the vertical arm of the “T” junction round the bend. A narrow-band analysis is presented in these results. We note that the numerical prediction agree reasonably well with the measured data. Both curves show similar interference patterns and of comparable magnitudes. We point out that the results shown in Figure 3 (e) are relatively poor compared with other results. It is because the receiver is placed in the vicinity of the corner at this configuration. The effect of the diffraction at the edge of the corner becomes more important for this particular case. Nevertheless, the agreement between numerical prediction and measured data is tolerable.

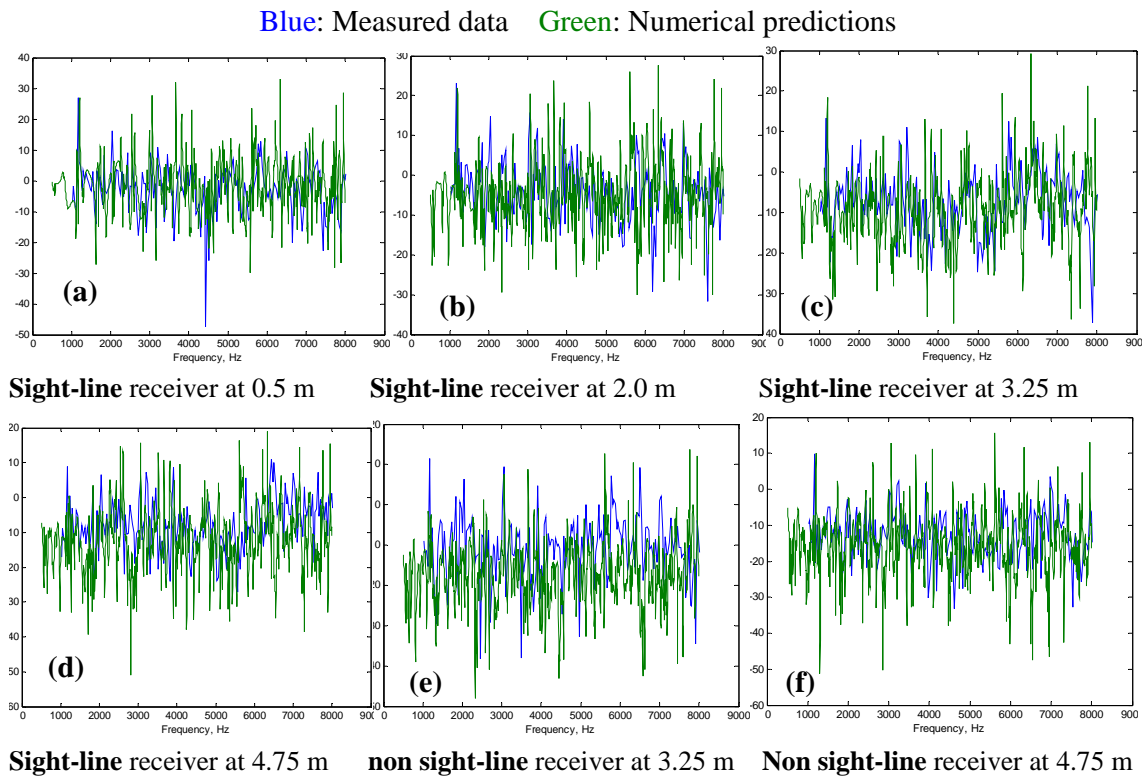


Figure 3: Comparison of the measured data with the predicted Relative Sound Pressure Levels (reference point at 0.25 m in front of the sound source) for different receiver positions. (a), (b), (c) and (d) for the sight line receiver located along the horizontal arm of the “T” junction. (e) and (f) for the sight-line receiver located at the vertical arm of the “T” junction.

Figure 4 shows comparisons of the predicted RSPL for receiver located at the sight-line and non sight-line round the bend. In both situations, the receivers were located at a total distance of 5 m from the source. Both results show a rather similar spectrum but the magnitudes of RSPL are different in both cases. This is because there is no direct field for the non sightline receiver. As expected, the sound fields are generally higher for a receiver placed along the line of sight than that for the non sight-line receiver of the same total distance.

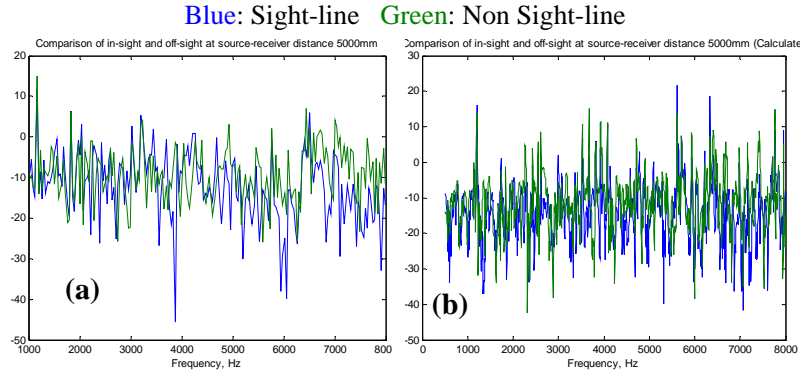


Figure 4. Comparison of predicted spectra for a sight-line and non sight-line receiver locating at a distance of 5 m from the source. (a) Measured data; (b) Numerical predictions.

3.2 Field measurements

Full-scale measurements were conducted to further validate the coherent model. Figure 5 shows the experimental setup of the field experiments which was in an enclosed T-shape corridor inside a building. The width and height of the corridor was 2.37m and 2.50m respectively. Both arms of the T-shaped corridor had a length longer than 15 m, and the length of the central corridor was 28m. The floor of the corridor was covered with a hard concrete surface. The walls were constructed with bricks finished a smooth layer of plaster covered with paints. The ceiling was constructed with gypsum boards along the whole length of the T-corridor. The floor and ceiling were treated effectively as flat and smooth surfaces. However, there were some recess areas along the boundary walls. The recess areas were used for the installation of doors of different rooms along the corridor. These vertical walls were also assumed to be hard smooth surfaces in order to simplify the numerical analysis. The background noise level was monitored throughout the experiments. Typically, the background noise level was around 40dBA the source signal had a level ranging from 85dBA to 95dBA. This signal level was significantly higher than the background. This precaution ensures that any adverse effect of background noise was minimized in all experimental measurements.

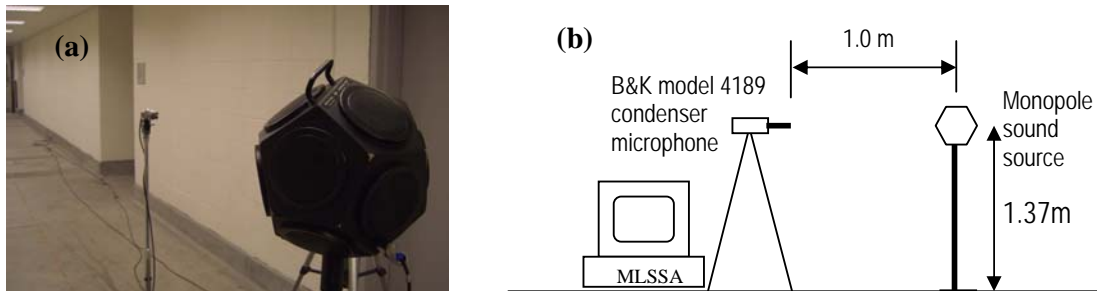


Figure 5: (a) The T- corridor enclosed in a building; (b) the schematic diagram of equipment used for field measurements.

As shown in Figure 5 (a), a Brüel and Kjør omni-directional speaker type 4296 was mounted at a height of 1.37m above ground and a Brüel and Kjør type 4189 ½” free field microphone were used respectively as the source and receiver. The microphone was also placed at the same height as the source during the measurements. Again, the same MLSSA was used both as a signal generator for the source and as an analyzer for the subsequent processing of data. In order to counter-check data of MLSSA, a B & K sound level meter is also used to record the one-third band sound pressure level at different receiver locations. In our experiments, the omni-directional speaker was placed at 10 m from the intersecting points of the centrelines of the perpendicular corridors, the recess area shown in Figure 5 (a). The first measurement point was located at 1.0m in front of the source. The successive receiver locations are set at a separation of 1.0 m either along the sight-line or round the corner of the “T” corridor. Each spectrum level was then normalized by the pre-recorded direct field measurement taken at 1 m from the source at the free field. The Excess Attenuation (EA) spectrum was obtained for comparison with numerical predictions.

Figure 6 (a) – (f) shows comparisons of the measured results with numerical predictions at various geometrical configurations, in one-third octave band spectrum. It can be noticed that both curves are of similar pattern. The maximum discrepancy between measured data and numerical predictions is about 5dB. For Figure 6(a), the receiver was located 2.0 m from the source. The direct sound field dominates the noise levels for this situation. Hence, the agreement between measurements and numerical predictions is the best among other configurations.

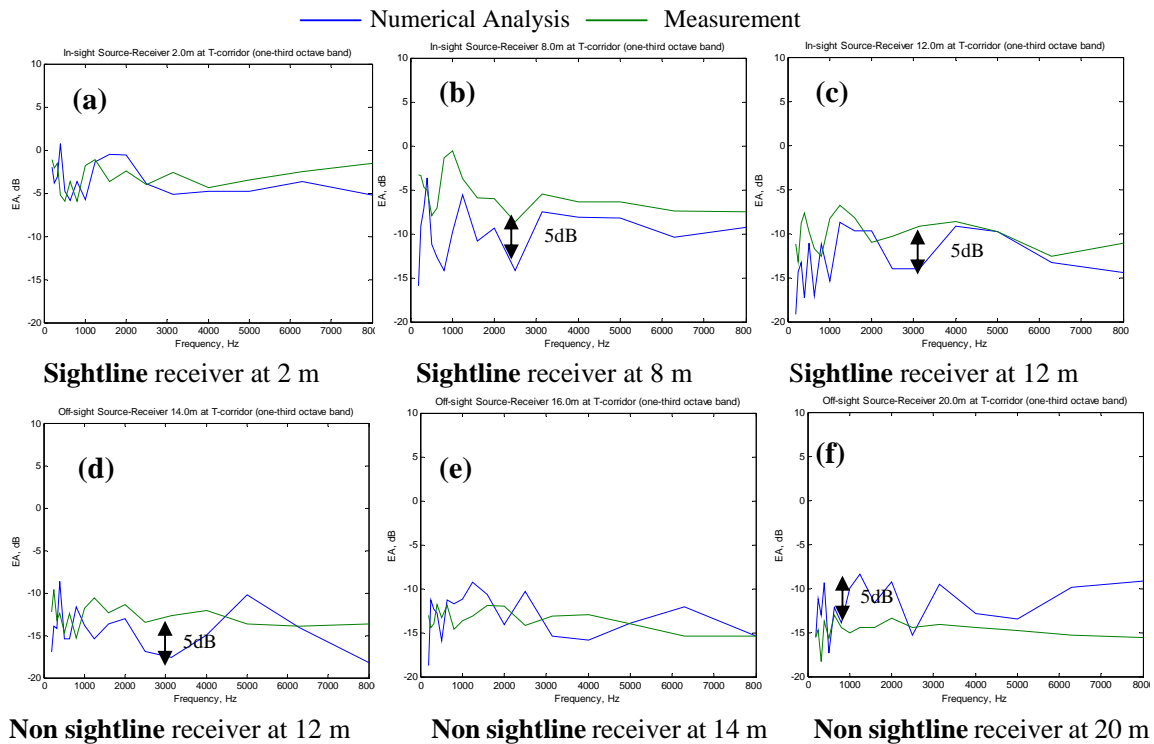


Figure 6: The above graphs show the comparison of the Measured and Calculated Excess Attenuation for different source-receiver distance

4. CONCLUSION

The image source method for the prediction of Excess Attenuation in a “T” corridor has been reported. The proposed image source method is validated by comparing it with a scale model

inside an anechoic chamber and a T-shape corridor inside a building. The theoretical prediction agrees tolerably well with the experimental results. Since the phase angle of each contributory ray is included in the numerical model, hence the model can give more accurate predictions of the interference effect which is in contrast with other energy-based approach.

4. ACKNOWLEDGEMENTS

The authors would like to thank Mr. C. N. Tang for technical supports. We wish to thank Mike Law, Chenly Lai and T. L. Yip for their in conducting the experiments. The authors gratefully acknowledge Dr. G. H. Frommer for his expert advise and the access of MTRC Depots.

REFERENCES

- [1] Sabine, W. C., "*Collected paper on Acoustics*," Harvard University Press, Cambridge, MA, 1927.
- [2] Eyring C. F., "Reverberation time in dead rooms," *Journal of the Acoustical Society of America* **1**, 217-241, (1930).
- [3] Millington G., "A modified formula for reverberation," *Journal of the Acoustical Society of America* **4**, 69-82, (1932).
- [4] Yamamoto, T., "On the distribution of sound in a corridor," *Journal of the Acoustical Society of Japan*, **17**, 286-292, (1961).
- [5] Allen J. B. and Berkeley D. A., "Image Method for efficient simulating small-room acoustics," *Journal of the Acoustical Society of America* **65**, 943-950, (1979).
- [6] Kutruff, K. H., "Sound decay in reverberation chamber with diffusing elements," *Journal of the Acoustical Society of America* **69** 1716-1723, (1981).
- [7] Redmore T. L., "A theoretical analysis and experimental study of the behaviour of sound in corridors," *Applied Acoustics* **15** 161-170, (1982).
- [8] Antonio J., Godinho L. and Tadeu A., "Reverberation times obtained using a numerical model versus those given by simplified formulas and measurements," *Acustica – Acta Acustica* **88**, 252 – 261, (2002).
- [9] Sergeev, M. V., "Scattered sound and reverberation on city streets and in tunnels", *Soviet Physics Acoustics* **25**, 248-252, (1979).
- [10] Barnett, P. W., "Acoustics of Underground Platforms", *Proceedings of the Institute of Acoustics* **16**(2), 433, (1994).
- [11] Gibbs C.G. and Jones D.K., "A Simple Image Method for calculating the distribution of Sound Pressure Levels within an Enclosure," *Acustica* **26**, 24-32, (1972).
- [12] Boish, J., "Extension of Image Model to arbitrary polyhedra", *Journal of the Acoustical Society of America* **75**, 1827-1836, (1984).
- [13] Dance S.M. and Shield B.M., "The Complete Image-Source Method For the Prediction of Sound Distribution in Non-Diffuse Enclosed Spaces," *Journal of Sound and Vibration* **201**, 473-489, (1997).
- [14] Dance S. M., Roberts J. P. and Shield B. M., "Computer prediction of sound distribution in enclosure spaces using an interference pressure model," *Applied Acoustics* **44**, 53-65, (1995).
- [15] Gensane M. and Santon F., "Prediction of Sound Fields in Rooms of Arbitrary shape: Validity of the Image Sources Method," *Journal of Sound and Vibration* **63**, 97-108, (1979).
- [16] Imaizumi H, Kunumatsu S., Isei T., "Sound propagation and speech transmission in a branching underground tunnel," *Journal of the Acoustical Society of America* **108**, 632-642, (2000).
- [17] Wang C. and Bradley J. S., "A Mathematical Model for a single screen barrier in open-plan Offices," *Applied Acoustics* **63**, 849-866, (2002).
- [18] Wang C. and Bradley J. S., "Prediction of the Speech Intelligibility Index behind a single screen in an open-plan Offices," *Applied Acoustics* **63**, 867-883, (2002).
- [19] Iu K. K. and Li K. M., "The propagation of sound in narrow street canyons," *Journal of the Acoustical Society of America* **112**, 537-550, (2002).
- [20] Li K.M., Iu K.K., "Propagation of sound in long enclosures," *Journal of the Acoustical Society of America* **116**, 2759-2770, (2004).
- [21] Li K.M., Iu K.K., "Transmission of noise in tunnels," *Journal of the Acoustical Society of America* **116**, 2759-2770 (2004).
- [22] T. F. W. Embleton, J. E. Piercy and N. Olson, "Outdoor sound propagation over ground of finite impedance," *Journal of the Acoustical Society of America* **59**, 267-277 (1976).